Unexpected Formation of Etheno-2‘-Deoxyguanosine Adducts from 5(S)-Hydroperoxyeicosatetraenoic Acid: Evidence for a Bis-Hydroperoxide Intermediate

ARTICLE *in* CHEMICAL RESEARCH IN TOXICOLOGY · APRIL 2005

Impact Factor: 3.53 · DOI: 10.1021/tx049693d · Source: PubMed

Unexpected Formation of Etheno-2′-Deoxyguanosine Adducts from 5(*S*)-Hydroperoxyeicosatetraenoic Acid: Evidence for a Bis-Hydroperoxide Intermediate

Wenying Jian,† Seon Hwa Lee,† Jasbir S. Arora,† Maria V. Silva Elipe,‡ and Ian A. Blair*,†

Center for Cancer Pharmacology, University of Pennsylvania School of Medicine, Philadelphia, Pennsylvania 19104-6160 and Analytical Sciences Department, Amgen, One Amgen, Center Drive, Thousand Oaks, California 91320

Received November 5, 2004

Analysis of products from the reaction between 5(*S*)-hydroperoxy-6,8,11,14-(*E*,*Z*,*Z*,*Z*)-eicosatetraenoic acid and 2′-deoxyguanosine in the presence of Fe^{II}, Fe^{III}, or vitamin C by liquid chromatography/atmospheric pressure chemical ionization/mass spectrometry revealed the presence of four DNA adducts. Surprisingly, adducts **I** and **II** had mass spectral characteristics identical to those for 1,N^2-etheno-2′-deoxyguanosine and heptanone-1,N^2-etheno-2′-deoxyguanosine. These adducts have previously been shown to arise from the homolytic decomposition of 13(*S*)-hydroperoxy-9,11-(*Z*,*E*)-octadecadienoic acid. It appears that under the reaction conditions, 5(*S*)-hydroperoxy-6,8,11,14-(*E*,*Z*,*Z*,*Z*)-eicosatetraenoic acid was subjected to a previously unknown peroxidation reaction to give a bis-hydroperoxide intermediate that underwent a Hock rearrangement to produce 3(*Z*)-nonenal from the ω-terminus. The 3(*Z*)-nonenal was then converted to 4-hydroperoxy-2-nonenal, a precursor to the formation of 4-oxo-2-nonenal. 4-Oxo-2-nonenal forms heptanone-1,N^2-etheno-adducts with 2′-deoxyguanosine, whereas 4-hydroperoxy-2-nonenal forms 1,N^2-etheno-2′-deoxyguanosine. Two novel carboxylate adducts were also identified. The structure of the more abundant adduct (**III**) was characterized as its methyl ester derivative by NMR spectroscopy as 3-(2′-deoxy-β-D-erythropentafuranosyl)-imidazo-7-(5″-carboxypenta-2″-one)-9-oxo[1,2-α]purine (5-carboxy-2-pentanone-1,N^2-etheno-2′-deoxyguanosine). This etheno adduct was formed by the reaction of 2′-deoxyguanosine with 5,8-dioxo-6(*E*)-octenoic acid. The bifunctional electrophile is proposed to arise from the α-terminus during the Hock rearrangement of bis-hydroperoxide derived from 5(*S*)-hydroperoxy-6,8,11,14-(*E*,*Z*,*Z*,*Z*)-eicosatetraenoic acid. 5-Carboxy-2-pentanone-1,N^2-etheno-2′-deoxyguanosine may serve as a biomarker of 5-lipoxygenase-mediated oxidative stress. The less abundant carboxylate adduct **IV** arose from a quite different pathway and was tentatively characterized as 6-carboxy-3-hydroxy-1-hexene-1,N^2-etheno-2′-deoxyguanosine.

Introduction

Polyunsaturated fatty acids (PUFAs)[1] can be converted into lipid hydroperoxides either by reactive oxygen species (ROS) (*1*) or by the action of lipoxygenases (LOXs) (*2*) and cyclooxygenases (COXs) (*3*). Lipid hydroperoxides undergo homolytic decomposition into bifunctional electrophiles, which react with DNA bases to form DNA adducts (*4*). These DNA modifications are proposed to be involved in the etiology of cancer, cardiovascular disease, and neurodegeneration (*4*, *5*). In previous studies, the homolytic decomposition of 13(*S*)-hydroperoxy-9,11-(*Z*,*E*)-octadecadienoic acid [13(*S*)-HpODE; a prototypic ω-6 PUFA lipid hydroperoxide] was examined. The major decomposition products were identified as 4-hydroperoxy-2-nonenal, 4-oxo-2-nonenal, 4-hydroxy-2-nonenal, and 4,5-epoxy-2(*E*)-decenal (*6*, *7*). 4-Oxo-2-nonenal was responsible for the formation of heptanone-1,N^6-etheno-2′-deoxyadenosine (heptanone-etheno-dAdo) and heptanone-1,N^2-etheno-2′-deoxyguanosine (heptanone-etheno-dGuo) adducts (*8*−*10*). 4-Hydroperoxy-2-nonenal and 4,5-epoxy-2(*E*)-decenal were the precursors in the formation of unsubstituted 1,N^6-etheno-dAdo (etheno-dAdo) and 1,N^2-etheno-dGuo (etheno-dGuo) adducts (*11*, *12*).

On the basis of structures of the bifunctional electrophiles, two pathways by which they were generated from 13(*S*)-HpODE were proposed (Scheme 1) (*13*). The first pathway, previously described by Pryor and Porter (*14*), was initiated by alkoxy radical formation through a one-electron reduction by vitamin C or a transition metal ion.

* To whom correspondence should be addressed. Fax: 215-573-9889. E-mail: ian@spirit.gcrc.upenn.edu.
† University of Pennsylvania School of Medicine.
‡ Amgen.

[1] Abbreviations: APCI, atmospheric pressure chemical ionization; CID, collision-induced dissociation; COSY, $^1H-^1H$ 2D correlation spectroscopy; COX, cyclooxygenase; dAdo, 2′-deoxyadenosine; d, doublet; dd, doublet of doublets; ddd, doublet of doublet of doublets; dGuo, 2′-deoxyguanosine; DIPE, diisopropylethylamine; etheno-dAdo, 1,N^6-etheno-2′-deoxyadenosine; etheno-dGuo, 1,N^2-etheno-2′-deoxyguanosine; HMBC, $^1H-^{13}C$ 2D heteronuclear multiple bond correlation; heptanone-etheno-dGuo, heptanone-1,N^2-etheno-2′-deoxyguanosine; HSQC, $^1H-^{13}C$ 2D heteronuclear single quantum correlation; 5(*S*)-HpETE, 5(*S*)-hydroperoxy-6,8,11,14-(*E*,*Z*,*Z*,*Z*)-eicosatetraenoic acid; 15-(*S*)-HpETE, 15(*S*)-hydroperoxy-5,8,11,13-(*E*,*Z*,*Z*,*Z*)-eicosatetraenoic acid; 13(*S*)-HpODE, 13(*S*)-hydroperoxy-9,11-(*Z*,*E*)-octadecadienoic acid; HRMS, high-resolution MS; LOX, lipoxygenase; m, multiplet; MOPS, 3-morpholinopropanesulfonic acid; PUFA, polyunsaturated fatty acid; ROE, rotating frame nuclear Overhauser effect; ROESY, rotating frame Overhauser enhancement spectroscopy; ROS, reactive oxygen species; s, singlet; TIC, total ion current.

10.1021/tx049693d CCC: $30.25
Published on Web 02/22/2005

Scheme 1. Mechanism of the Formation of 4-Hydroperoxy-2-nonenal, 4-Oxo-2-nonenal, 4-Hydroxy-2-nonenal, and *trans*-4,5-Epoxy-2(*E*)-decenal from 13(*S*)-HpODE

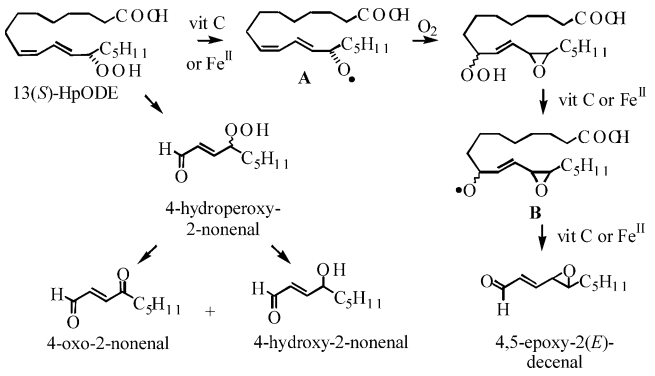

Alkoxy radial **A** rearranged to form an epoxide with concomitant addition of molecular oxygen and then one-electron reduction to give the intermediate **B**, which then underwent an α-cleavage to form *trans*-4,5-epoxy-2(*E*)-decenal (Scheme 1). The other pathway involved the formation of 4-hydroperoxy-2-nonenal as the intermediate, which underwent dehydration to 4-oxo-2-nonenal or reduction into 4-hydroxy-2-nonenal (Scheme 1).

Arachidonic acid is an essential fatty acid and a precursor of leukotrienes, which are potent extracellular mediators of inflammation and allergic disorders (*15*). The first step of biosynthesis of leukotrienes is conversion of arachidonic acid into 5(*S*)-hydroperoxy-6,8,11,14-(*E*,*Z*,*Z*,*Z*)-eicosatetraenoic acid [5(*S*)-HpETE] by 5-LOX. In this study, the dGuo adducts produced from the reaction between 5(*S*)-HpETE and dGuo in the presence of transition metal ion or vitamin C were characterized by LC/MS and NMR analysis.

Materials and Methods

Materials. Ammonium acetate, ammonium iron(III) sulfate dodecahydrate, ammonium iron(II) sulfate hexahydrate, vitamin C, *N*-bromosuccinimide, citric acid, 2′-deoxyguanosine (dGuo), dichloromethane, *N*,*N*′-dicyclohexylcarbodiimide, diisopropylethylamine (DIPE), 4-dimethylaminopydridine, ethyl acetate, hydrochloric acid, *N*-methyl-*N*-nitroso-*p*-toluensulfonamide, pyridine, sodium chloride, sodium hydroxide, sodium sulfate, and sodium thiosulfate were from Sigma-Aldrich (St. Louis, MO). 5(*S*)-HpETE was from Cayman Chemical (Ann Arbor, MI) or from the reaction of potato 5-LOX with arachidonic acid. 15-(*S*)-Hydroperoxy-(*E*,*Z*,*Z*,*Z*)-5,8,11,13-eicosatetraenoic acid [15-(*S*)-HpETE], potato 5-LOX, and arachidonic acid were from Cayman Chemical. 3-Morpholinopropanesulfonic acid (MOPS) was from Fluka BioChemika (Milwaukee, WI). Chelex-100 chelating ion exchange resin (100−200 mesh size) was from Bio-Rad Laboratories (Hercules, CA). HPLC grade water, acetonitrile, ethanol, hexane, methanol, 2-propanol, and tetrahydrofuran were from Fisher Scientific Co. (Fair Lawn, NJ). Methyl-^{13}C iodide was from Cambridge Isotope Laboratories Inc. (Andover, MA), and gases were from BOC Gases (Lebanon, NJ).

LC. Chromatography for LC/MS experiments was performed using a Waters Alliance 2690 HPLC system (Waters Corp., Milford, MA). Preparation of the adducts for NMR analysis was conducted on a Hitachi L-6200A Intelligent Pump (Hitachi, San Jose, CA) equipped with a SpectroMonitor 3000 UV detector (LDC/Milton Roy, Riviera Beach, FL). Systems 1 and 2 employed a YMC-Pack ODS-AQ column (250 mm × 4.6 mm i.d., 5 μm). Systems 3 and 4 employed a YMC-Pack ODS-AQ column (250 mm × 10.0 mm i.d., 5 μm). System 5 employed a Phenomenex Luna C18 column (250 mm × 10.0 mm i.d., 5 μm). For systems 1−3, solvent A was 5 mM ammonium acetate in water and solvent B was 5 mM ammonium acetate in acetonitrile. For systems 4 and 5, solvent A was water and solvent B was acetonitrile. The gradient for system 1 was as follows: 60% B at 0 min, 60% B at 15 min, 100% B at 20 min, 100% B at 25 min, 60% B at 27 min, and 60% B at 35 min. The gradient for system 2 was as follows: 6% B at 0 min, 6% B at 3 min, 20% B at 9 min, 20% B at 13 min, 40% B at 20 min, 80% B at 21 min, 80% B at 24 min, 6% B at 26 min, and 6% B at 34 min. The gradient for system 3 was as follows: 6% B at 0 min, 6% B at 3 min, 20% B at 9 min, 20% B at 13 min, 40% B at 20 min, 80% B at 21 min, 80% B at 24 min, 6% B at 26 min, and 6% B at 34 min. System 4 employed an isocratic mobile phase of 20% B. The gradient for system 5 was as follows: 6% B at 0 min, 6% B at 3 min, 20% B at 9 min, 20% B at 13 min, 60% B at 21 min, 80% B at 22 min, 80% B at 30 min, 6% B at 32 min, and 6% B at 45 min. Flow rates were 1 mL/min for systems 1 and 2 and 2.5 mL/min for systems 3−5. Gradient elution was conducted in linear mode, and all separations were performed at ambient temperature.

MS. MS was conducted with a Thermo Finnigan LCQ ion trap mass spectrometer (Thermo Finnigan, San Jose, CA) equipped with an atmospheric pressure chemical ionization (APCI) source in positive ion mode. The LCQ operating conditions were as follows: vaporizer temperature was 450 °C, heated capillary temperature was 150 °C, with a discharge current of 5 μA applied to the corona needle. Nitrogen was used as the sheath (80 psi) and auxiliary (10 units) gas to assist with nebulization. Full scanning analyses were performed in the range of *m/z* 50 to *m/z* 800. Collision-induced dissociation (CID) experiments coupled with multiple tandem mass spectrometry (MS^n) employed helium as the collision gas. The relative collision energy was set at 35% of the maximum (1 V).

NMR. Spectra were determined at 27 °C (300 K) on a Bruker Avance 600 instrument equipped with a Bruker 2.5 mm multinuclear inverse *z*-gradient probe. ^{1}H and ^{13}C experiments were carried out at 600.13 and 150.92 MHz, respectively. The samples (0.5−2 mg) were dissolved in 150 μL of DMSO-d_6. The data processing was performed on the spectrometer. Chemical shifts are reported in the δ scale (ppm) by assigning the residual solvent peak to 2.50 and 39.51 ppm for DMSO for ^{1}H and ^{13}C, respectively. The rotating frame nuclear Overhauser effect (ROE) experiments were determined with a 300 ms mixing time for the one-dimensional (1D) selective ROE and with 200 and 300 ms mixing times for the two-dimensional (2D) rotating frame Overhauser enhancement spectroscopy (ROESY) experiments. The delays between successive pulses were 1 and 2 s for ^{1}H−^{1}H 2D correlation spectroscopy (COSY) and ROESY, respectively. Both the ^{1}H−^{13}C 2D heteronuclear single quantum correlation (HSQC) and the ^{1}H−^{13}C 2D heteronuclear multiple bond correlation (HMBC) spectra were determined using gradient pulses for coherence selection. The HSQC spectrum was determined with decoupling during acquisition. Delays corresponding to one bond ^{13}C−^{1}H coupling (ca. 145 Hz) for the low-pass filter and to 2−3 bond ^{13}C−^{1}H long-range coupling (5, 7, or 10 Hz) were used for the HMBC.

5(*S*)-HpETE. The purity of our synthetic 5(*S*)-HpETE and commercially obtained 5(*S*)-HpETE was examined by reversed phase LC/MS using gradient system 1. A single chromatographic peak was observed at a retention time of 22.7 min. The mass spectrum contained a dominant dehydrated molecular ion $[M - H_2O + H]^+$ at *m/z* 319, together with the following major fragment ions: $[M - H_2O_2 + H]^+$ at *m/z* 303, $[M - H_2O + NH_4]^+$ at *m/z* 336, and $[M + NH_4]^+$ at *m/z* 354. These LC/MS analyses confirmed that the 5(*S*)-HpETE was >99% pure.

Fe^{II}-Mediated Decomposition of 5(*S*)-HpETE or 15(*S*)-HpETE in the Presence of dGuo. A solution of 5(*S*)-HpETE or 15(*S*)-HpETE (50 μg, 149 nmol) in ethanol (10 μL) and $FeSO_4(NH_4)_2SO_4{\cdot}6H_2O$ (234 μg, 596 nmol) in water (10 μL) was added to dGuo (159 μg, 596 nmol) in Chelex-treated 100 mM MOPS containing 150 mM NaCl (pH 7.4, 180 μL). The reaction mixture was sonicated for 15 min at room temperature and

incubated at 60 °C for 24 h. An aliquot of the sample (20 μL) was analyzed by LC/MS using gradient system 2.

Methylation of the Reaction Products. Ethereal diazomethane was prepared by reacting *N*-methyl-*N*-nitroso-*p*-toluensulfonamide with sodium hydroxide, employing a diazomethane generator from Wheaton (Millville, NJ). A portion of reaction mixture (100 μL) was evaporated under a stream of nitrogen, dissolved in 100 μL of methanol, and then mixed with 1 mL of freshly prepared ethereal diazomethane. The reaction was conducted at room temperature for 1 h and terminated by evaporating the solvent under nitrogen. The methylated reaction mixture was redissolved with 100 μL of water, and 20 μL of the sample was applied to LC/MS analysis using gradient system 2.

Synthesis of 5,8-Dioxo-6(*E*)-octenoic Acid. To a solution of 4-(2-furyl)butanoic acid (*16*) (308 mg, 2 mmol) and pyridine (633 mg, 4 mmol) in tetrahydrofuran−acetone−H_2O (5:4:1, 6 mL) was added *N*-bromosuccinimide (320 mg, 4 mmol) dissolved in tetrahydrofuran−acetone−H_2O (5:4:1, 2 mL) at −20°C. The solution was stirred for 1 h at −20°C and then poured into a mixture of ethyl acetate and aqueous sodium thiosulfate. The organic layer was separated and washed with aqueous citric acid solution (pH 3). The organic layer was dried and evaporated under reduced pressure. The residue was purified on a silica gel column using ethyl acetate in hexane to afford pure 5,8-dioxo-6(*E*)-octenoic acid (60 mg, 33%). ^{1}H NMR (500 MHz, $CDCl_3$, δ): 1.99 (p, J = 7.5 Hz, 2H, CH_2), 2.44 (t, J = 7.5 Hz, 2H, CH_2), 2.80 (t, J = 7.5 Hz, 2H, CH_2), 6.79 (dd, J = 7, 16 Hz, 1H, CH), 6.88 (d, J = 16 Hz, 1H, CH), 9.78 (d, J = 7 Hz, 1H, OCH). High-resolution MS (HRMS) calculated for $C_8H_{10}O_4$ (MH^+) 171.065734; found, 171.065599.

Reaction of 5,8-Dioxo-6(*E*)-octenoic Acid with dGuo. A solution of 5,8-dioxo-6(*E*)-octenoic acid (153 μg, 900 nmol) in ethanol (6 μL) was added to dGuo (160 μg, 600 nmol) in Chelex-treated 100 mM MOPS containing 150 mM NaCl (pH 7.4, 194 μL). The reaction mixture was sonicated for 15 min at room temperature and incubated at 60 °C for 24 h. An aliquot of the sample (20 μL) was analyzed by LC/MS using gradient system 2.

Synthesis of Methyl-4-(2-furyl)butanoate. *N*,*N*′-Dicyclohexylcarbodiimide (824 mg, 4 mmol) was added to a well-stirred solution of 4-(2-furyl)butanoic acid (*16*) (308 mg, 2 mmol), 4-dimethylaminopydridine (25 mg, 0.2 mmol), and methanol (192 mg, 6 mmol) in dichloromethane (15 mL). The reaction mixture was stirred for 2 h under an atmosphere of nitrogen and then filtered. The filtrate was washed with water followed by brine and dried over anhydrous sodium sulfate. The organic layer was evaporated, and the residue was purified by column chromatography to afford methyl-4-(2-furyl)butanoate (250 mg, 74%). ^{1}H NMR ($CDCl_3$, 500 MHz): δ 1.97 (q, J = 7.5 Hz, 2H), 2.35 (t, J = 7.5 Hz, 2H), 2.67 (t, J = 7.5 Hz, 2H), 3.66 (s, 3H), 6.00 (d, J = 2.5 Hz, 1H), 6.26 (d, J = 2 Hz, 1H), 7.29 (m, 1H). HRMS calculated for $C_9H_{12}O_3$ (MH^+), 168.078644; found, 168.079006.

Synthesis of Methyl-5,8-dioxo-6(*E*)-octenoate. *N*-Bromosuccinimide (318 mg, 1.77 mmol) dissolved in tetrahydrofuran−acetone−H_2O (5:4:1, 2 mL) was added to a solution of methyl 4-(2-furyl)butanoate (250 mg, 1.48 mmol) and pyridine (353 mg, 4.44 mmol) in tetrahydrofuran−acetone−H_2O (5:4:1, 6 mL) at −20 °C. The solution was stirred for 1 h at −20 °C and 6 h at room temperature and then poured into a mixture of ethyl acetate and aqueous sodium thiosulfate. The organic layer was separated and washed with aqueous citric acid solution (pH 3). The organic layer was dried and evaporated under reduced pressure. The residue was purified on a silica gel column using ethyl acetate in hexane to afford methyl-5,8-dioxo-6(*E*)-octenoate (90 mg, 33%). ^{1}H NMR ($CDCl_3$, 500 MHz): δ 1.99 (q, J = 7.5 Hz, 2H), 2.40 (t, J = 7.5 Hz, 2H), 2.79 (t, J = 7.5 Hz, 2H), 3.68 (s, 3H), 6.78 (dd, J = 7, 16 Hz, 1H), 6.86 (d, J = 16 Hz, 1H), 9.78 (d, J = 7 Hz, 1H). HRMS calculated for $C_9H_{12}O_4$ (MH^+), 185.081384; found, 185.081365.

Reaction of Methyl-5,8-dioxo-6(*E*)-octenoate with dGuo. A solution of methyl-5,8-dioxo-6(*E*)-octenoate with dGuo (27.4 μg, 149 nmol) in ethanol (10 μL) and 10 μL of water was added to dGuo (159 μg, 596 nmol) in Chelex-treated 100 mM MOPS containing 150 mM NaCl (pH 7.4, 180 μL). The reaction mixture was sonicated for 15 min at room temperature and incubated at 60 °C for 24 h. An aliquot of the sample (20 μL) was analyzed by LC/MS using gradient system 2.

Preparation of Methyl-III and ^{13}C-Methylated Methyl-III for NMR Analysis. (i) A solution of methyl-5,8-dioxo-6(*E*)-octenoate (8.5 mg, 50 μmol) in ethanol (50 μL) was added to dGuo (66.7 mg, 250 μmol) in Chelex-treated 100 mM MOPS containing 150 mM NaCl (pH 7.4, 10 mL). The reaction mixture was sonicated for 15 min at room temperature and incubated at 60 °C for 24 h. The reaction products were isolated by preparative HPLC using gradient system 3. The reaction products were fraction-collected, combined, and concentrated under nitrogen. Secondary purification was conducted using gradient system 4 to furnish pure methyl-**III** (7.4 mg, 38%). (ii) To a solution of methyl-**III** (3.0 mg, 6.93 μmol) in acetonitrile (6.67 mL), a solution of 20% (v/v) DIPE in acetonitrile (1340 μL) and a solution of methyl-^{13}C iodide (492 mg, 3.5 mmol) in acetonitrile (1340 μL) were added. The reaction mixture was sonicated for 5 min at room temperature and incubated at room temperature for 1 h. The reaction was stopped by evaporation under nitrogen, and the reaction mixture was dissolved in 6.67 mL of 50% (v/v) acetonitrile in water. The reaction products were isolated by preparative HPLC using gradient system 5. The reaction products were fraction-collected, combined, and concentrated under nitrogen to give pure ^{13}C-methylated-methyl-**III** (1.0 mg, 32%).

Fe^{III}-Mediated Decomposition of 5(*S*)-HpETE in the Presence of dGuo. A solution of 5(*S*)-HpETE (50 μg, 149 nmol) in ethanol (10 μL) and $FeNH_4(SO_4)_2 \cdot 12H_2O$ (287.39 μg, 596 nmol) in water (10 μL) was added to dGuo (159 μg, 596 nmol) in Chelex-treated 100 mM MOPS containing 150 mM NaCl (pH 7.4, 180 μL). The reaction mixture was sonicated for 15 min at room temperature and incubated at 60 °C for 24 h. An aliquot of the sample (20 μL) was analyzed by LC/MS using gradient system 2.

Vitamin C-Mediated Decomposition of 5(*S*)-HpETE in the Presence of dGuo. A solution of 5(*S*)-HpETE (50 μg, 149 nmol) in ethanol (10 μL) and vitamin C (104.96 μg, 596 nmol) in water (10 μL) was added to dGuo (159 μg, 596 nmol) in Chelex-treated 100 mM MOPS containing 150 mM NaCl (pH 7.4, 180 μL). The reaction mixture was sonicated for 15 min at room temperature and incubated at 60 °C for 24 h. An aliquot of the sample (20 μL) was analyzed by LC/MS using gradient system 2.

Results

Fe^{II}-Mediated Decomposition of 5(*S*)-HpETE in the Presence of dGuo. LC/MS analysis of the reaction products between 5(*S*)-HpETE and dGuo at 60 °C for 24 h indicated the presence of four DNA adducts (Figure 1). Adduct **I** eluted at 9.7 min (Figure 1D) with an MH^+ at *m/z* 292 together with a fragment ion at *m/z* 176 corresponding to the protonated modified base (B) to which an additional proton had been transferred (BH_2^+) (Figure 2A; upper). LC/MS analysis of methylated adduct **I** showed a change in retention time to 12.4 min (Figure 3D) and revealed an MH^+ at *m/z* 306 with a BH_2^+ ion at *m/z* 190 (Figure 2A; lower). This indicated that monomethylation had occurred. The LC/MS characteristics of adduct **I** and its monomethyl derivative were identical to those of etheno-dGuo, an adduct derived from *trans*-4,5-epoxy-2(*E*) decenal (*11*) and 4-hydroperoxy-2-nonenal (*12*), major homolytic decomposition products of 13(*S*)-HpODE.

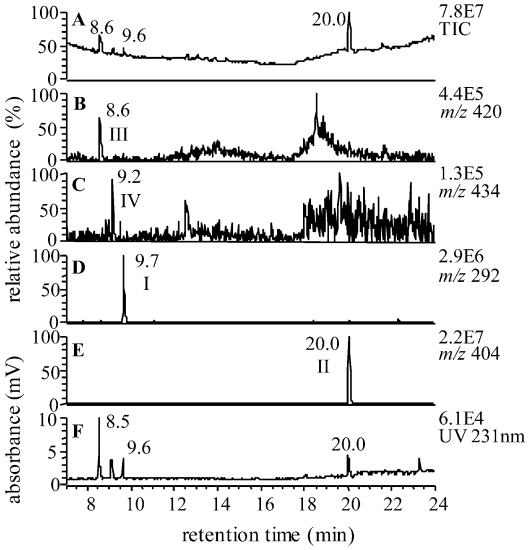

Figure 1. LC/MS analysis of reaction products between 5(*S*)-HpETE and dGuo mediated by Fe^{II} using system 2. (A) Total ion current (TIC) chromatogram. (B) Reconstructed ion chromatogram for MH^+ of adduct **III** (*m/z* 420, 8.6 min). (C) Reconstructed ion chromatogram for MH^+ of adduct **IV** (*m/z* 434, 9.2 min). (D) Reconstructed ion chromatogram for MH^+ of adduct **I** (*m/z* 292, 9.7 min). (E) Reconstructed ion chromatogram for MH^+ of adduct **II** (*m/z* 404, 20.0 min). (F) UV absorbance at 231 nm.

Adduct **II** eluted at 20.0 min (Figure 1E) with an MH^+ at *m/z* 404 and a BH_2^+ ion at *m/z* 288 (Figure 2B; upper). Upon methylation, its retention time shifted to 21.4 min (Figure 3E). An MH^+ at *m/z* 418 and a BH_2^+ ion at *m/z* 302 were observed (Figure 2B; lower). This suggested that monomethylation had occurred to adduct **II**. The LC/MS characteristics of adduct **II** and its monomethyl derivative were identical to those for heptanone-etheno-dGuo, a major product from the reaction of 13(*S*)-HpODE with dGuo (*8*). The UV response at 231 nm for monomethyl adduct **I** was much higher than that for the monomethyl derivative of adduct **II** (Figure 3F).

Adduct **III** eluted at 8.6 min (Figure 1B) with an MH^+ at *m/z* 420 and a BH_2^+ ion at *m/z* 304 (Figure 4A; upper). Adduct **IV** eluted at 9.2 min (Figure 1C) with an MH^+ at *m/z* 434 and a BH_2^+ ion at *m/z* 318 (Figure 4B; upper). Methylation increased the MS response of adducts **III** and **IV** by more than a factor of 10. The retention time of adduct **III** shifted to 18.4 min (Figure 3B) with an MH^+ at *m/z* 448 and a BH_2^+ ion at *m/z* 332 (Figure 4A; lower). The retention time of adduct **IV** shifted to 19.5 min (Figure 3C) with an MH^+ at *m/z* 462 and a BH_2^+ ion at *m/z* 346 (Figure 4B; lower). These data were consistent with bis-methylation of adducts **III** and **IV**.

Fe^{II}-Mediated Decomposition of 15(*S*)-HpETE in the Presence of dGuo. LC/MS analysis of the reaction products between 15(*S*)-HpETE and dGuo at 60 °C for 24 h revealed two adducts, which were identical to those produced by reaction between 5(*S*)-HpETE and dGuo (data not shown). The mass spectrum of the most abundant adduct (**II**, 20.0 min) showed an intense MH^+ at *m/z* 404, together with a BH_2^+ ion at *m/z* 288. This corresponded to heptanone-etheno-dGuo. The other adduct (**I**, 9.7 min) showed a molecular ion MH^+ at *m/z* 292 and a BH_2^+ at *m/z* 176, corresponding to etheno-dGuo. The relative abundances of adduct **I** and adduct **II** produced by 5(*S*)-HpETE were 75 and 96%, respectively, of those produced by 15(*S*)-HpETE under the same conditions.

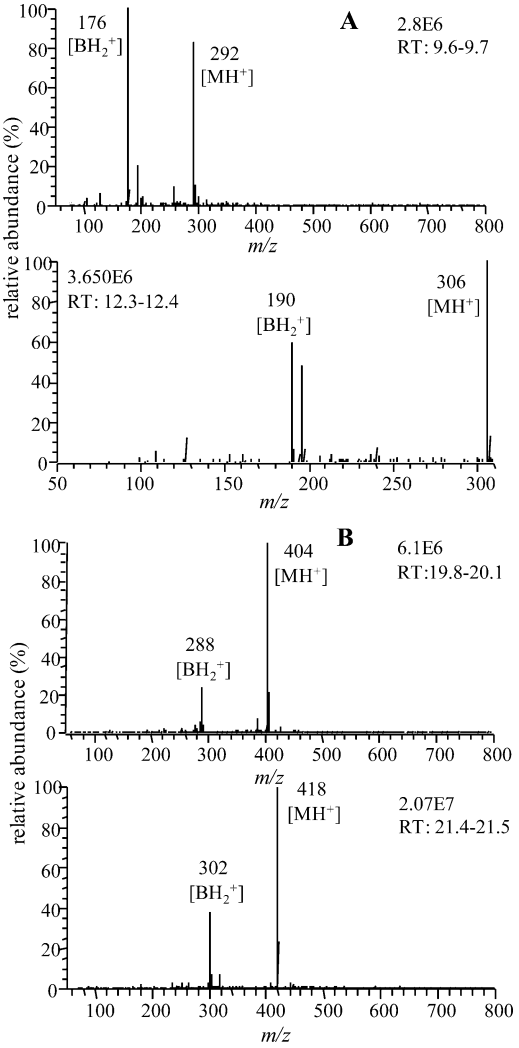

Figure 2. Mass spectra of dGuo adducts from reaction between 5(*S*)-HpETE and dGuo mediated by Fe^{II}. (A) Mass spectra of adduct **I** before methylation (upper) and after methylation (lower). (B) Mass spectra of adduct **II** before methylation (upper) and after methylation (lower).

Reaction of 5,8-Dioxo-6(*E*)-octenoic Acid with dGuo. The proposed precursor of adduct **III**, 5,8-dioxo-6(*E*)-octenoic acid, was synthesized and reacted with dGuo. The reaction mixture was then analyzed by LC/MS. The resulting chromatogram showed the presence of one major product, which eluted at 8.6 min (Figure 5 upper) with an MH^+ ion at *m/z* 420 and a BH_2^+ ion at *m/z* 304 (Figure 5 lower). These LC/MS properties were identical to adduct **III** derived from the reaction between 5(*S*)-HpETE and dGuo (Figures 1B and 4A upper). MS^2 analyses were conducted for this major product (Figure 6A) and for adduct **III** derived from the reaction between 5(*S*)-HpETE and dGuo (Figure 6B). Their mass spectra were identical. MS^2 analysis of *m/z* 420 resulted in formation of the BH_2^+ product ion at *m/z* 304, together with a minor ion at *m/z* 286 ($-H_2O$).

Reaction of Methyl-5,8-dioxo-6(*E*)-octenoate with dGuo. To facilitate structural NMR studies of adduct **III**, 5,8-dioxo-6(*E*)-octenoic acid was synthesized as its methyl ester derivative (methyl-5,8-dioxo-6(*E*)-octenoate) and reacted with dGuo. LC/MS analysis showed the presence of one major adduct (methyl-**III**), which eluted at 13.1 min (Figure 7A) with an MH^+ ion at *m/z* 434 and BH_2^+ ion at *m/z* 318 (Figure 7B). The reaction mixture was

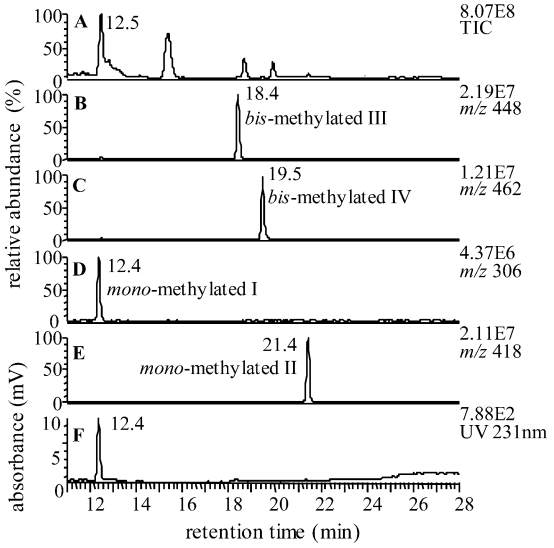

Figure 3. LC/MS analysis of methylated reaction products from Fe^{II}-mediated decomposition of 5(*S*)-HpETE and dGuo using system 2. (A) TIC chromatogram. (B) Reconstructed ion chromatogram for MH^+ of bis-methylated adduct **III** (*m/z* 448, 18.4 min). (C) Reconstructed ion chromatogram for MH^+ of bis-methylated adduct **IV** (*m/z* 462, 19.5 min). (D) Reconstructed ion chromatogram for MH^+ of monomethylated adduct **I** (*m/z* 306, 12.4 min). (E) Reconstructed ion chromatogram for MH^+ of monomethylated adduct **II** (*m/z* 418, 21.4 min). (F) UV absorbance at 231 nm.

then methylated with diazomethane and subjected to LC/MS analysis. The major product eluted at 18.4 min (Figure 7C) with an MH^+ ion at *m/z* 448 and BH_2^+ ion at *m/z* 332 (Figure 7D), showing an identical retention time (18.4 min; Figure 3B) and identical MS properties (Figure 4A; lower) to bis-methylated adduct **III** derived from the reaction between 5(*S*)-HpETE and dGuo. Coinjection of the bis-methylated products derived from 5(*S*)-HpETE and methyl-5,8-dioxo-6(*E*)-octenoate revealed a single peak eluted at 18.4 min with an MH^+ at *m/z* 448 (data not shown).

LC/MS^n Analysis of Methyl Derivatives of Adduct III. MS^n analyses were conducted for three compounds: (i) the methyl derivative of the major product from the reaction between dGuo and 5,8-dioxo-6(*E*)-octenoic acid, (ii) the methyl derivative of the major product from the reaction between dGuo and methyl-5,8-dioxo-6(*E*)-octenoate, and (iii) the bis-methyl derivative of adduct **III** from the reaction between 5(*S*)-HpETE and dGuo. The methyl derivatives from each reaction showed the same retention time on the LC system (18.4 min), and their mass spectra were identical. Each MH^+ appeared at *m/z* 448 (Figure 8A). MS^2 analysis of *m/z* 448 resulted in the almost exclusive formation of the BH_2^+ product ion at *m/z* 332 (Figure 8B). CID of *m/z* 332 (MS^3) gave rise to the product ion at *m/z* 300 ($-CH_3OH$) (Figure 8C). Finally, CID of the ion at *m/z* 300 (MS^4) gave rise to an ion at *m/z* 258 ($-COCH_2$) (Figure 8D). MS^3 revealed the presence of a carboxyl group, and MS^4 was consistent with the presence of a pentanone moiety.

LC/MS^n Analysis of the Methyl Derivative of Adduct IV. The poor positive ionization characteristics of underivatized adduct **IV** resulted in a very weak signal when analyzed by LC/APCI/MS (Figure 1). However, after methylation with diazomethane, the signal from adduct **IV** increased in intensity by almost 2 orders of magnitude. LC/APCI/MS analysis revealed an MH^+ at

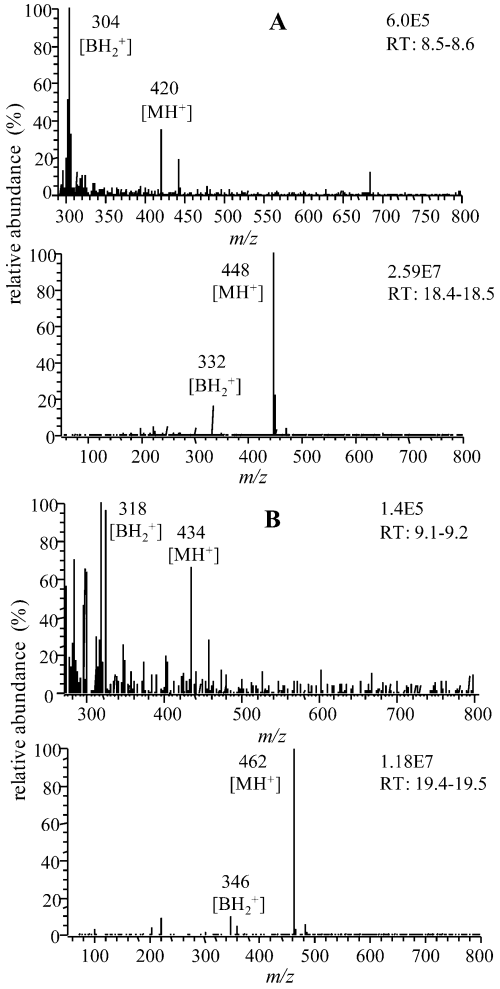

Figure 4. Mass spectra of dGuo adducts from Fe^{II}-mediated decomposition of 5(*S*)-HpETE in the presence of dGuo. (A) Adduct **III** before methylation (upper) and after methylation (lower). (B) Adduct **IV** before methylation (upper) and after methylation (lower).

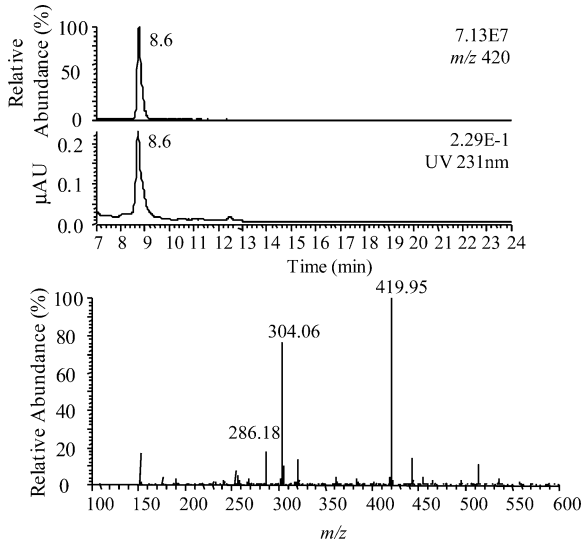

Figure 5. LC/MS analysis of reaction products between 5,8-dioxo-6(*E*)-octenoic acid and dGuo using system 2. The upper panel shows the reconstructed ion chromatogram for MH^+ of the adduct (*m/z* 420, 8.6 min). The middle panel shows the UV absorbance at 231 nm. The lower panel shows the mass spectrum of the adduct (adduct **III**).

m/z 462 showing that bis-methylation had occurred (Figure 9A). This was most likely due to *N*-methylation

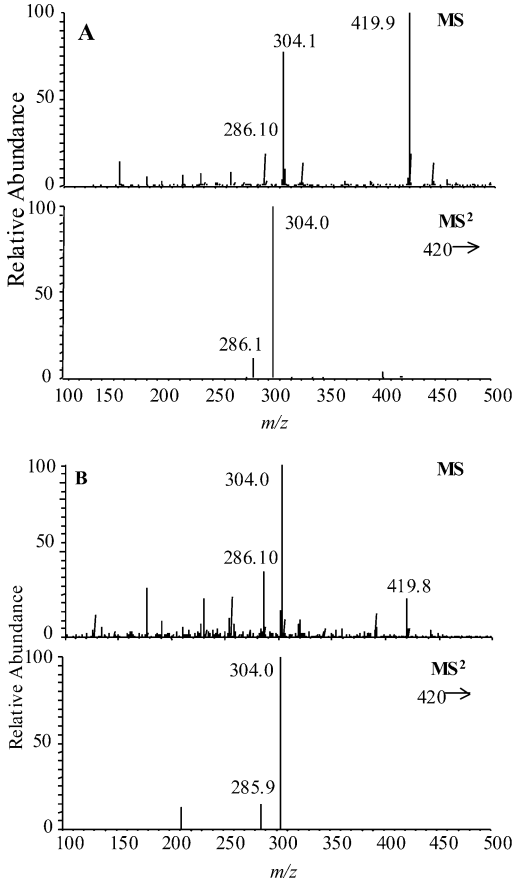

Figure 6. (A) MS^1 and MS^2 analyses of the major product from the reaction of 5,8-dioxo-6(*E*)-octenoic acid with dGuo. (B) MS^1 and MS^2 analyses of adduct **III**.

(as was observed with adduct **III**) in addition to formation of the expected methyl ester derivative (Scheme 5). Analysis by LC/MS^n confirmed the initial loss of the 2′-deoxyribose moiety from MH^+ (*m/z* 462) on CID to give a typical BH_2^+ ion at *m/z* 346 (Figure 9B). MS^3 of *m/z* 346 provided a major product ion at *m/z* 314 corresponding to the loss of CH_3OH from the methyl ester (Figure 9C), together with ions at *m/z* 296 ($-CH_3OH-H_2O$), 268 ($-CH_3OH-H_2O-CO$), and 202 ($-CH_3OH-H_2O-CO-C_3H_2N_2$). MS^4 analysis of *m/z* 314 (Figure 9D), *m/z* 296 (Figure 9E), and *m/z* 268 (Figure 9F) revealed that these ions were precursors of product ions *m/z* 296, 268, and 202, respectively. An additional minor ion was observed at *m/z* 230 in the MS^4 spectrum of *m/z* 314 (Figure 9D). This ion appeared to result from initial loss $C_3H_2N_2$ (66 Da) from the imidazole portion of the adduct in a manner similar to the ion that appeared at *m/z* 202. This was followed by the loss of H_2O from the hexenyl side chain to give a product ion at *m/z* 230. None of the intermediate that would result from the simple loss of $C_3H_2N_2$ (at *m/z* 248) was detected. It is noteworthy that an ion derived from the loss of $C_3H_2N_2$ was the only ion observed during MS^n analysis once the hexenyl side chain had undergone dehydration (Figure 9F). Thus, MS^n spectra were consistent with the 6-carboxymethyl-1-hexenyl-etheno-*N*-methyl-dGuo structure shown in Scheme 5. However, the structural assignment of the bis-methyl derivative of adduct **IV** as well as the underivatized form of adduct **IV** can only be considered tentative at this stage.

NMR Analysis of Methyl-III. The reaction product between dGuo and methyl-5,8-dioxo-6(*E*)-octenoate was purified and subjected to NMR analysis. The aromatic proton singlet at 7.00 ppm (H-6) (Figure 10 and Table 1) showed a COSY correlation with the methylene protons at C-1″ (4.10 and 4.06 ppm) (Figure 11). This confirmed the presence of an olefinic bond between C-6 and C-7, which was further confirmed by the ^{13}C NMR spectrum (Table 2). The NMR data were consistent with four possible structures for the carboxymethylpentanone-etheno-dGuo adduct, shown as methyl-**IIIA**–**D** in Scheme 2. The triplet at 2.58 ppm was assigned to the methylene protons at C-3″ based on its chemical shift and its multiplicity (Table 1). The COSY spectrum showed correlations between the C-3″ protons with the C-4″

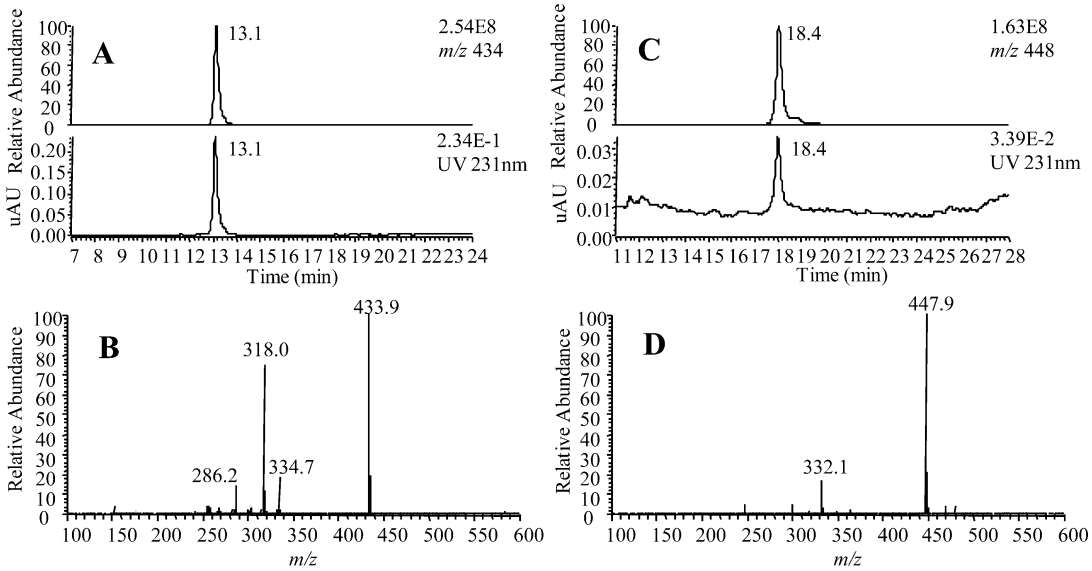

Figure 7. (A) LC/MS analysis of reaction products between methyl-5,8-dioxo-6(*E*)-octenoate and dGuo using system 2. The upper panel shows the reconstructed ion chromatogram for MH^+ of the major adduct (*m/z* 434, 13.1 min). The lower panel shows the UV absorbance at 231 nm. (B) Mass spectrum of the major product from the reaction of methyl-5,8-dioxo-6(*E*)-octenoate with dGuo. (C) LC/MS analysis of the adduct from the reaction between methyl-5,8-dioxo-6(*E*)-octenoate and dGuo after methylation with diazomethane using system 2. The upper panel shows the reconstructed ion chromatogram for MH^+ of the adduct (*m/z* 448, 18.4 min). The lower panel shows the UV absorbance at 231 nm. (D) Mass spectrum of the major product from the reaction between methyl-5,8-dioxo-6(*E*)-octenoate and dGuo after methylation with diazomethane.

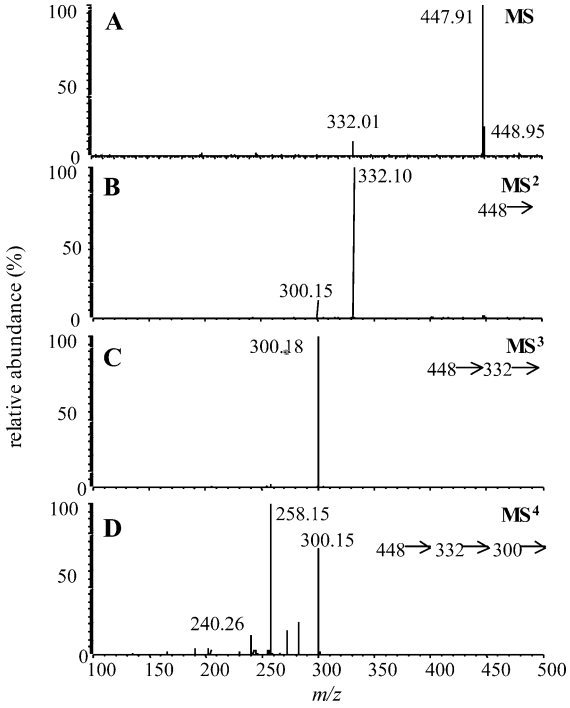

Figure 8. MS^n analyses of the bis-methyl derivative of the product from reaction between dGuo and 5,8-dioxo-6(*E*)-octenoic acid. (A) MS^1, (B) MS^2, (C) MS^3, and (D) MS^4.

protons (1.75 ppm) and, finally, the C-4″ protons and the C-5″ protons (2.32 ppm). The COSY spectrum also showed the correlations of the protons of the furanosyl moiety. This spectrum showed correlations between proton H-1′ (6.21 ppm) and the protons at C-2′ (2.64 and 2.20 ppm), the C-2′ protons with the C-3′ proton (4.37 ppm), the C-3′ protons with the C-4′ proton (3.85 ppm), and the C-4′ proton with the C-5′ protons (3.59 and 3.52 ppm) (Figure 11). The ROESY spectrum indicated rotation of the N3−C1′ bond based on the NOEs between protons at C-2 with H-1′ and H-2′ of the furanosyl moiety. The ^1H and ^{13}C chemical shifts by HSQC of the methyl group (3.58 and 51.4 ppm, respectively) were indicative of the methyl ester of the side chain moiety. HMBC was carried out at three different long-range C−H coupling constants (J = 5, 7, and 10 Hz) to avoid missing correlations. Assignments of C-1a (116.0 ppm), C-3a (150.2 ppm), and C-4a (148.5 ppm) through the H-2/C-1a, H-2,1′/C-3a, and H-6/C-4a HMBC correlations were essential for this analysis. Unfortunately, these data could not distinguish between the four proposed structures of methyl **IIIA**−**D** (Scheme 2). Therefore, the [^{13}C]-methyl derivative of methyl-**III** was prepared to avoid ambiguous assignments. Its ^1H NMR spectrum showed the labeled methyl group as a doublet with a coupling constant of 141.5 Hz (Table 3) and as a singlet (31.4 ppm) in the ^{13}C NMR spectrum (data not shown). A 1D ROE experiment irradiating at 7.21 ppm (H-6) elicited ROE signals from H-1″ (4.15 and 4.12 ppm) and the labeled N−$^{13}CH_3$ (d, 3.61, J = 141.5 Hz) indicating that the labeled methyl group was attached to the nitrogen at position 5 and the methyl ester side chain moiety was attached to position 7 of the imidazopurine ring. The HMBC experiment (Figure 12) showed that the ^{13}C signal of the [^{13}C]methyl group correlated to its own protons and to H-6 indicating that it was attached to the N-5, three bonds away. On the basis of these data, the structure for the carboxymethylpentanone-etheno-dGuo was assigned as methyl-**IIIA** {3-(2′-deoxy-β-D-erythropentafuranosyl)imidazo-7-(5″-methylcarboxypenta-2″-one)-9-oxo-[1,2-α]purine}. The structure of the [^{13}C]methyl-**IIIA** was assigned as 3-(2′-deoxy-β-D-erythropentafuranosyl)imidazo-7-(5″-methylcarboxypenta-2″-one)-5-N-[^{13}C]methyl-9-oxo[1,2-α]purine.

Fe^{III}-Mediated Decomposition of 5(*S*)-HpETE in the Presence of dGuo. LC/MS analysis of the reaction products formed between 5(*S*)-HpETE and dGuo in the presence of 3 mM Fe^{III} at 60 °C for 24 h indicated the same product profile as the reactions mediated by 3 mM Fe^{II} (data not shown).

Vitamin C-Mediated Decomposition of 5(*S*)-HpETE in the Presence of dGuo. LC/MS analysis of the reaction products formed between 5(*S*)-HpETE and dGuo in the presence of 3 mM vitamin C at 60 °C for 24 h showed the same product profile as the reactions mediated by 3 mM Fe^{II} (data not shown).

Discussion

5-LOX is the enzyme responsible for the formation of 5(*S*)-HpETE in vivo. It is expressed primarily in leukocytes, including monocytes and macrophages (*15*). Recent studies have implicated the 5-LOX pathway as an important mediator in the pathology of atherosclerosis. For example, 5-LOX is present in macrophages in atherosclerotic lesions (*17*) and the 5-LOX gene is shown to be a major atherosclerosis susceptibility locus in mice (*18*). Our previous studies on the homolytic decomposition

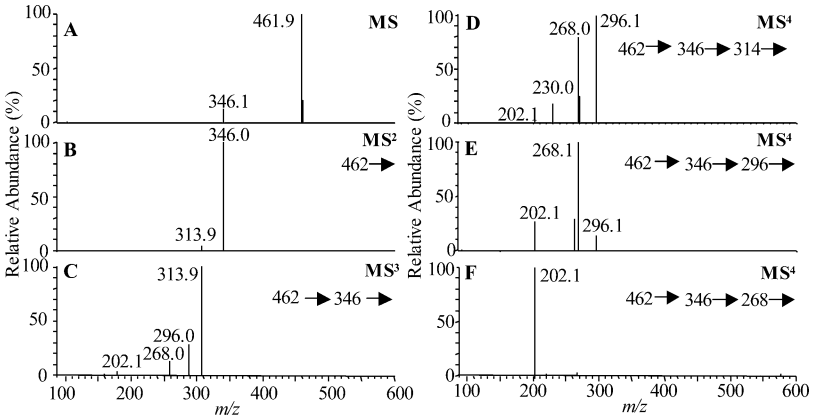

Figure 9. MS^n analyses of the bis-methyl derivative of adduct **IV**. (A) MS. (B) MS^2 analysis of *m/z* 462. (C) MS^3 analysis of *m/z* 346. (D) MS^4 analysis of *m/z* 314. (E) MS^4 analysis of *m/z* 296. (F) MS^4 analysis of *m/z* 268.

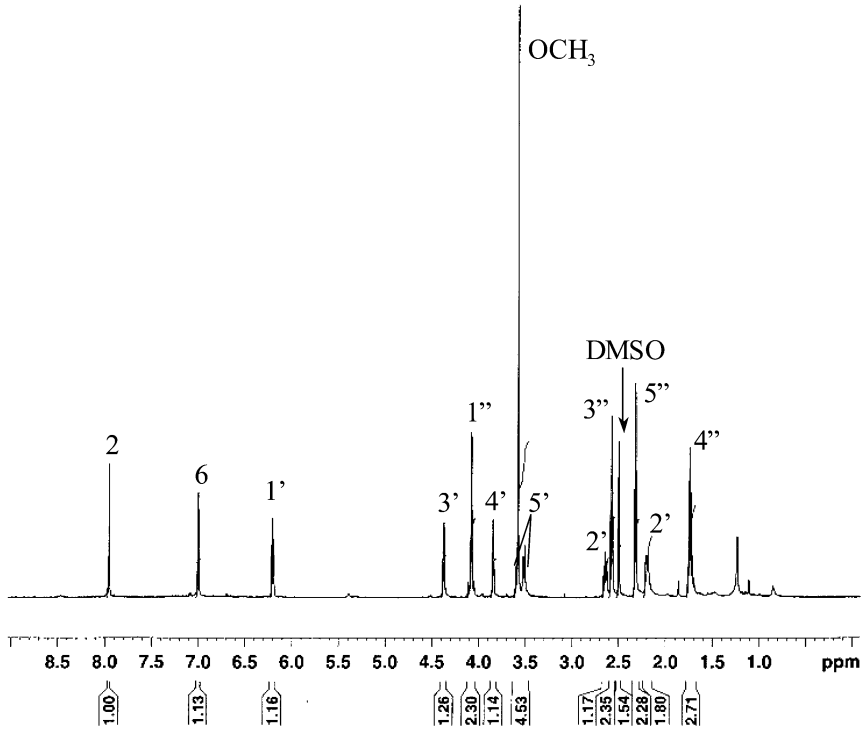

Figure 10. ^{1}H NMR spectrum of methyl-**III** in DMSO-d_6.

Table 1. ^{1}H NMR Assignments for Methyl-IIIA[a]

assigned H	δ (ppm)	multiplicity	H-coupled (J Hz)	type
H-2	7.95	s		N=C*H*−
H-6	7.00	s	H-1″	C=C*H*
H-1′	6.21	t	H-2′a (6.9), H-2′b (6.9)	N−C*H*−O
H-3′	4.37	m	H-2′a, H-2′b, H-4′	−O−C*H*−
H-1″b	4.10	d	H-1″a (17.8)	−CH_2−C
H-1″a	4.06	d	H-1″b (17.8)	−CH_2−C
H-4′	3.85	m	H-3′, H-5′a, H-5′b	−O−C*H*−
H-5′b	3.59	m	H-4′, H-5′a	−CH_2−O
OCH_3	3.58	s		−COOCH_3
H-5′a	3.52	m	H-4′, H-5′b	−CH_2−O
H-2′b	2.64	m	H-1′, H-2′a, H-3′	−CH_2−C
H-3″a,b	2.58	t	H-4″a (7.2), H-4″b (7.2)	−CH_2−C
H-5″a,b	2.32	t	H-4″a (7.5), H-4″b (7.5)	−CH_2−C
H-2′a	2.20	m	H-1′, H-2′b, H-3′	−CH_2−C
H-4″a,b	1.74	m	H-3″a,b, H-5″a,b	−CH_2−C

[a] Spectra were obtained in DMSO-d_6.

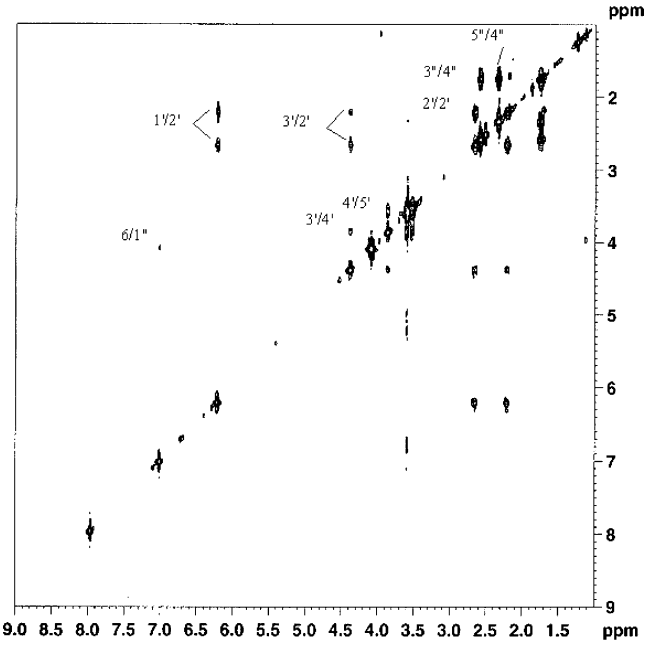

Figure 11. Two-dimensional ^{1}H−^{1}H COSY spectrum of methyl-**III** in DMSO-d_6.

of 13(*S*)-HpODE (*7*−*11*) suggested that DNA adducts would be formed through homolytic decomposition of 5(*S*)-HpETE. We hypothesized that the adducts would be formed through a 4-oxo-2-nonenal-like molecule that contained the carboxy terminus and that the adducts would initiate apoptosis, a pathway known to be involved in atherosclerosis (*19*, *20*). Studies of Hankin et al. (*21*) have already established that carboxylate-containing DNA adducts could be formed from leukotriene A_4, another 5-LOX-derived product. Therefore, it was very surprising that two of the products derived from the homolytic decomposition of 5(*S*)-HpETE in the presence of dGuo were etheno-dGuo and heptanone-etheno-dGuo, respectively. These were the major adducts, and they had previously been characterized as the major products from the homolytic decomposition of 13(*S*)-HpODE in the presence of dGuo. They clearly arose from the ω-terminus of the PUFA lipid hydroperoxide. 15(*S*)-HpETE has the same ω-terminal structure as that of 13(*S*)-HpODE, and so, we originally suspected that the production of etheno-dGuo and heptanone-etheno-dGuo had resulted from contamination by 15(*S*)-HpETE. This could have been formed as a contaminant during the preparation of 5(*S*)-HpETE. However, LC/MS analysis confirmed that the 5(*S*)-HpETE was >99% pure. Furthermore, the amount of etheno-dGuo and heptanone-etheno-dGuo formed from 15(*S*)-HpETE was similar to that formed from 5(*S*)-HpETE. This suggested that the etheno adducts had arisen by a previously unrecognized pathway of 5(*S*)-HpETE decomposition.

Our earlier studies established that heptanone-etheno-dGuo is formed from 4-oxo-2-nonenal (*8*), which in turn arises through decomposition of 4-hydroperoxy-2-non-

Table 2. ^{13}C NMR Assignments for Methyl-IIIA[a]

assigned carbon	δ (ppm)	coupling	type
C-4″	18.7	H-3″, H-5″	−*C*H$_2$−
C-5″	32.7	H-3″, H-4″, OCH$_3$	−*C*H$_2$−
C-2′	39.7	H-4′	−*C*H$_2$−
C-1″	40.0	H-6	−*C*H$_2$−
C-3″	40.4	H-4″, H-5″	−*C*H$_2$−
O−CH$_3$	51.4		COO−*C*H$_3$
C-5′	62.1	H-3′	−*C*H$_2$−O
C-3′	71.1	H-2′, H-4′, H-5′	−*C*H−O
C-1′	83.6	H-2′, H-3′, H-4′	N−*C*HO−
C-4′	88.1	H-2′, H-3′, H-5′	−*C*HO
C-1a	116.0	H-2	C=*C*−N
C-7	117.3	H-1″, H-6	C=*C*−N
C-6	118.9	H-1″	−N−*C*H=C
C-2	136.7	H-1′	−N−*C*H=N
C-4a	148.5	H-6	−N−*C*=N
C-3a	150.2	H-2, H-1′	N−*C*=N
C-9	154.5[b]	H-2	=*C*O
C-6″	173.4	H-4″, H-5″, OCH$_3$	−*C*OOCH$_3$
C-2″	206.0	H-1″, H-3″, H-4″	−*C*=O

[a] Spectra were obtained in DMSO-d_6. [b] Tentative assignment.

Scheme 2. Possible Structures for Methyl-III

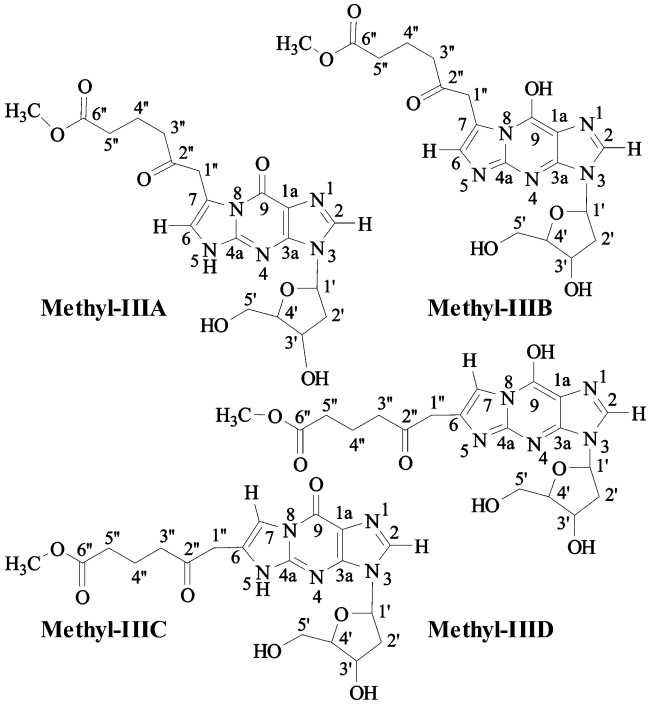

enal. It has been suggested that formation of 4-hydroperoxy-2-nonenal from 13(*S*)-HpODE is initiated by abstraction of an allylic hydrogen atom to form a carbon-centered radical at C-8 (*22*). Addition of molecular oxygen at the allylic C-10 carbon atom then results in the formation of a 10,13-bis-hydroperoxide, which undergoes a Hock rearrangement to give 4-hydroperoxy-2-nonenal (*22*, *23*). An analogous reaction with 5(*S*)-HpETE would result in the formation of a carbon-centered radical at C-10 (Scheme 3). In fact, this reaction would be even more favorable than with 13(*S*)-HpODE because the hydrogen atoms at C-10 are bis-allylic. It is noteworthy that the bis-allylic hydrogen atoms are also targets for radical-mediated abstraction during peroxidation of PUFAs (*1*). The hydrogen abstraction could be mediated by either alkoxy or peroxy radicals, which are formed in the presence of transition metal ions or vitamin C. The carbon-centered radical at C-10 would then undergo allylic addition of molecular oxygen at C-12 to give an

Table 3. ^{1}H NMR Assignments for the [^{13}C]methyl Derivative of Methyl-IIIA[a]

assigned H	δ (ppm)	multiplicity	H-coupled (J Hz)	type
H-2	8.08	s		N=C*H*−
H-6	7.21	s		C=C*H*
H-1′	6.28	t	H-2′a (7.0), H-2′b (7.0)	N−C*H*−O
H-3′	4.40	m	H-2′a, H-2′b, H-4′	−O−C*H*−
H-1″b	4.15	d	H-1″a (18.6)	−C*H*$_2$−C
H-1″a	4.12	d	H-1″b (18.6)	−C*H*$_2$−C
H-4′	3.86	m	H-3′, H-5′a, H-5′b	−O−C*H*−
N-^{13}CH$_3$	3.61	d	^{13}CH$_3$ (141.5)	−N−C*H*$_3$
H-5′b	3.60	m	H-4′, H-5′a	−C*H*$_2$−O
O−CH$_3$	3.59	s		−COOC*H*$_3$
H-5′a	3.52	m	H-4′, H-5′b	−C*H*$_2$−O
H-2′b	2.67	ddd	H-1′ (7.7), H-2′a (13.2), H-3′ (5.7)	−C*H*$_2$−C
H-3″a,b	2.62	t	H-4″a (7.2), H-4″b (7.2)	−C*H*$_2$−C
H-5″	2.33	t	H-4″a (7.5), H-4″b (7.5)	−C*H*$_2$−C
H-2′a	2.24	ddd	H-1′ (6.1), H-2′b (13.2), H-3′ (2.9)	−C*H*$_2$−C
H-4″a,b	1.76	m	H-3″a, H-3″b, H-5″a, H-5″b	−C*H*$_2$−C

[a] Spectra were obtained in DMSO-d_6.

intermediate 5,12-bis-hydroperoxide. A Hock rearrangement (*23*−*25*) then results in the formation of 3(*Z*)-nonenal, an unstable aldehyde that rapidly forms 4-hydroperoxy-2-nonenal (*26*). The resulting 4-hydroperoxy-2-nonenal gives rise to 4-oxo-2-nonenal, which forms heptanone-etheno adducts with dGuo (*8*). The unsubstituted etheno-dGuo arises from the reaction of 4-hydroperoxy-2-nonenal with dGuo (*12*).

During LC/MS analysis, two additional adducts were observed (adduct **III** and adduct **IV**). Adduct **III** showed an MH$^+$ at *m/z* of 420 and a BH$_2^+$ ion at *m/z* 304 (Figure 4A) and eluted with a relatively short retention time (8.6 min) on reverse phase HPLC analysis (Figure 1B). Methylation increased the retention time to 18.4 min and increased its MS response significantly (Figure 3B), indicating adduct **III** contained a polar carboxylate moiety. The proposed precursor of adduct **III**, 5,8-dioxo-6(*E*)-octenoic acid was synthesized and reacted with dGuo. The reaction product showed identical retention time (Figure 5 upper), molecular ion (Figure 5 lower), and MS^2 properties (Figure 6A) to those of adduct **III** (Figures 1B, 4A, and 6B).

To confirm the structure of adduct **III**, the methyl ester of 5,8-dioxo-6(*E*)-octenoic acid was synthesized and reacted with dGuo. The resulting methyl ester analogue of adduct **III** (methyl-**III**) was then subjected to extensive NMR analysis. These studies indicated that there were four possible structures for methyl-**III** (methyl-**IIIA**−**D**; Scheme 2). To unequivocally assign the regioselectivity of dGuo addition to methyl-5,8-dioxo-6(*E*)-octenoate, a [^{13}C]methyl derivative of methyl-**III** was prepared. ^{1}H NMR analysis showed the ^{13}C-methyl group protons as a doublet with a coupling constant of 141.5 Hz (Table 3) and the ^{13}C-methyl as a singlet at 31.4 ppm in the ^{13}C NMR spectrum. A 1D ROE experiment was conducted in which H-6 at 7.21 ppm was irradiated. This resulted in ROE signals from H-1″ at 4.15 and 4.12 ppm as well as the protons attached to the ^{13}C at 3.61 ppm (d, J = 141.5 Hz). These studies confirmed that the labeled methyl group was attached to N-5 and that the methyl ester side chain moiety was attached to C-7 of the imidazopurine ring. Finally, an HMBC experiment showed that the ^{13}C-methyl group correlated to its own protons and to H-6 (three bonds away) confirming that it was

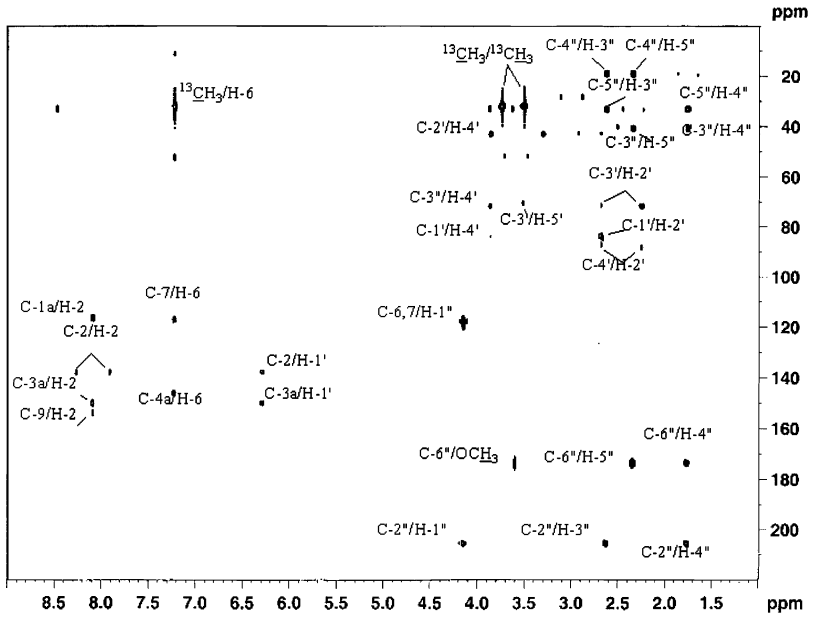

Figure 12. $^1H-^{13}C$ HMBC spectrum of [^{13}C]methyl-methyl-**III** in DMSO-d_6.

Scheme 3. Proposed Mechanism for the Formation of Etheno-dGuo, Heptanone-etheno-dGuo, and Carboxypentanone-etheno-dGuo from the Reaction between 5(*S*)-HpETE and dGuo

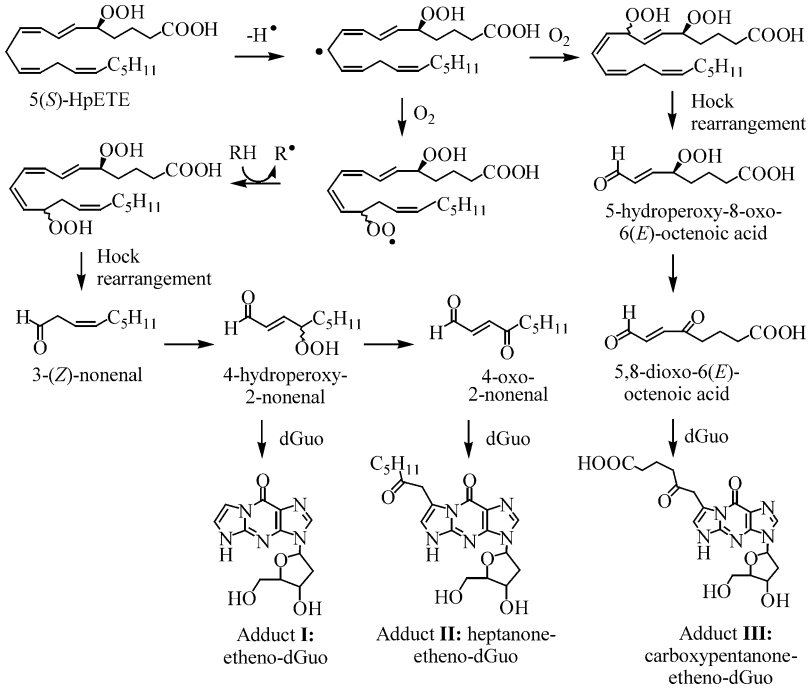

attached to N-5 (Figure 12). These data provided unequivocal evidence that carboxymethylpentanone-etheno-dGuo, derived from methyl-5,8-dioxo-6-octenoci acid, was 3-(2′-deoxy-β-D-erythropentafuranosyl)imidazo-7-(5″-methylcarboxypenta-2″-one)-5-N-[^{13}C]methyl-9-oxo[1,2-α]-purine (methyl-**IIIA**; Scheme 2).

Carboxypentanone-etheno-dGuo derived from the reaction of dGuo with 5,8-dioxo-6(*E*)-octenoic acid had identical LC/MS properties with carboxypentanone-etheno-dGuo prepared from the reaction of dGuo with 5(*S*)-HpETE (Scheme 4). The bis-methylated derivative of adduct **III** prepared from methylation of carboxypentanone-etheno-dGuo had identical LC/MS properties to the bis-methylated derivative of carboxypentanone-etheno-dGuo prepared from the reaction of dGuo with 5(*S*)-HpETE. Finally, the LC/MS properties of both bis-methylated derivatives were identical to the methyl derivative of carboxymethylpentanone-etheno-dGuo prepared from the reaction of methyl-5,8-dioxo-6-(*E*)-octenoic acid with dGuo (Scheme 4). This established that the regioselectivity of addition to dGuo was the same as that observed with dGuo and 4-oxo-2-nonenal (*8*). Initial nucleophilic attack occurs from the exocyclic dGuo amino group N^2 at the C-8 aldehyde of 5,8-dioxo-6(*E*)-octenoic acid. Subsequent Michael addition of the N1 pyrimidine to C-7 of the resulting carbinolamine intermediate is followed by dehydration to the etheno-dGuo adduct **III** (Scheme 3). We suggest that 5,8-dioxo-6(*E*)-octenoic acid arises by a mechanism that is similar to that proposed previously for the formation of 9,12-dioxo-10-dodecenoic acid from 13(*S*)-HpODE (*23*). The carbon-centered radical at C-10 undergoes allylic addition of molecular oxygen

Scheme 4. Formation of Mono- and Bis-methylated Carboxypentanone-etheno-dGuo

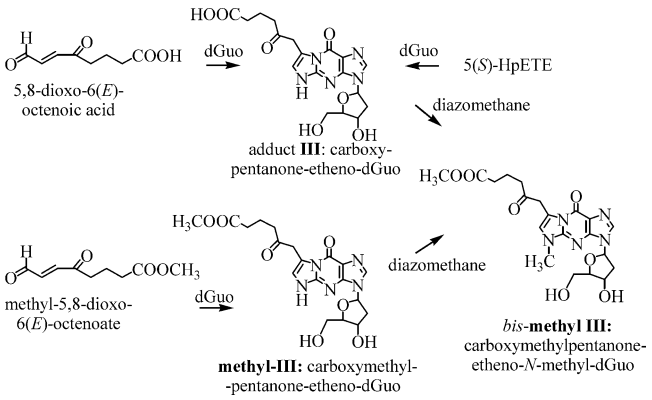

Scheme 5. Proposed Scheme for Formation of Adduct IV and Assignment of MS^n Product Ions from Bis-methyl IV, Tentatively Identified as 6-Carboxymethyl-3-hydroxy-1-hexenyl-etheno-*N*-methyl-dGuo

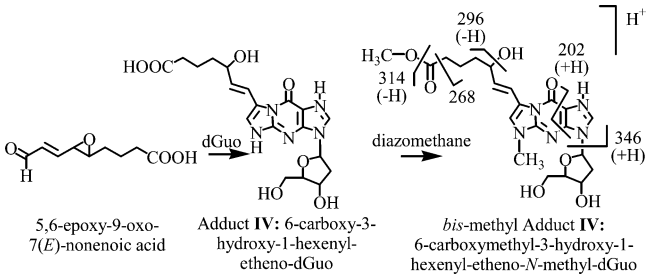

at C-8 to form a 5,8-bis-hydroperoxide (Scheme 3). A Hock rearrangement of the hydroperoxide C-8 results in the formation of 5-hydroperoxy-8-oxo-6(*E*)-octenoic acid, a carboxylate-containing analogue of 4-hydroperoxy-2-nonenal (*12*). By analogy with the reaction of 4-hydroperoxy-2-nonenal, this is then converted to 5,8-dioxo-6(*E*)-octenoic acid, the precursor to the formation of adduct **III** (5-carboxy-2-pentanone-etheno-dGuo).

Adduct **IV** was the less abundant carboxylate-containing adduct from the reaction of 5(*S*)-HpETE with dGuo. The adduct had an MH^+ at *m/z* 434 and a BH_2^+ ion at *m/z* 318 (Figure 4B) with a relatively short retention time of 9.2 min (Figure 1C) on the reversed phase HPLC system. The retention time of adduct **IV** was significantly prolonged to 19.5 min after bis-methylation (Figure 3C), indicating that the adduct contained a carboxyl group. On the basis of the mass spectral data of underivatized adduct **IV** (Figure 4B) and its bis-methyl derivative (Figure 9), adduct **IV** was tentatively identified as 6-carboxy-3-hydroxy-1-hexenyl-etheno-dGuo, derived from 5,6-epoxy-9-oxo-7(*E*)-nonenoic acid (Scheme 5). We suggest that the formation of 5,6-epoxy-9-oxo-7(*E*)-nonenoic acid from 5(*S*)-HpETE could occur by a mechanism previously described by Pryor and Porter (*14*), analogous to the formation of 4,5-epoxy-2(*E*)-decenal from 13(*S*)-HpODE.

In separate studies, it was demonstrated that Fe^{II}, Fe^{III}, or vitamin C could initiate the homolytic decomposition of 5(*S*)-HpETE with similar efficacy. Fe^{II} or vitamin C cause a one-electron reduction of the hydroperoxide to produce alkoxy radicals (*27*, *28*), which can readily abstract one of the bis-methylene hydrogen atoms in the 1,4-pentadiene system of PUFAs (*29*). It is proposed that under the reaction conditions, the alkoxy radicals serve either as initiators or as intermediates in the free radical chain reaction (Scheme 3). In the case of Fe^{III}, it is suggested that Fe^{III} reacts with the lipid hydroperoxide to produce peroxy radicals, which cause free radical chain reactions by hydrogen abstraction. Fe^{III} itself is reduced to Fe^{II}, which then initiates a one-electron reduction of the lipid hydroperoxides. This explains why the reaction profiles are similar for Fe^{II}, Fe^{III}, and vitamin C.

In summary, 5-LOX-mediated oxidation of arachidonic acid can lead to the formation of etheno-DNA adducts. If not repaired, DNA adducts may induce apoptosis (*30*). Indeed, it has been shown that there is increased DNA damage in atherosclerotic lesions (*31*), and apoptotic macrophages in atherosclerotic lesions show signs of DNA synthesis and repair, implying that DNA damage has occurred in these cells (*32*). The carboxypentanone-etheno-dGuo adduct identified in the present study could potentially induce apoptosis due to the bulky polar carboxyl group that is present. Therefore, these results provide a possible link between 5-LOX activity, DNA damage, and apoptosis. Furthermore, the carboxylate-containing etheno adduct may serve as a specific biomarker for 5-LOX-mediated DNA damage in vivo. The consequences resulting from formation of heptanone-etheno-dGuo and unsubstituted etheno-dGuo adducts are not clear at this time. Unsubstituted etheno adducts have been linked with mutagenesis and carcinogenesis rather than apoptosis (*33*, *34*). However, the surprising formation of these adducts has provided new mechanistic insight into the homolytic decomposition of lipid hydroperoxides.

Acknowledgment. We acknowledge financial support from NIH Grants RO1-CA91016 and P50-HL70128.

References

(1) Porter, N. A., Caldwell, S. E., and Mills, K. A. (1995) Mechanisms of free radical oxidation of unsaturated lipids. *Lipids 30*, 277−290.

(2) Brash, A. R. (1999) Lipoxygenases: Occurrence, functions, catalysis, and acquisition of substrate. *J. Biol. Chem. 274*, 23679−23682.

(3) Laneuville, O., Breuer, D. K., Xu, N., Huang, Z. H., Gage, D. A., Watson, J. T., Lagarde, M., DeWitt, D. L., and Smith, W. L. (1995) Fatty acid substrate specificities of human prostaglandin-endoperoxide H synthase-1 and -2. *J. Biol. Chem. 270*, 19330−19336.

(4) Blair, I. A. (2001) Lipid hydroperoxide-mediated DNA damage. *Exp. Gerontol. 36*, 1473−1481.

(5) Spiteller, G. (2001) Lipid peroxidation in aging and age-dependent disease. *Exp. Gerontol. 36*, 1425−1457.

(6) Lee, S. H., and Blair, I. A. (2000) Characterization of 4-oxo-2-nonenal as a novel product of lipid peroxidation. *Chem. Res. Toxicol. 13*, 698−702.

(7) Lee, S. H., Oe, T., and Blair, I. A. (2001) Vitamin C-induced decomposition of lipid hydroperoxides to endogenous genotoxins. *Science 292*, 2083−2086.

(8) Rindgen, D., Nakajima, M., Wehrli, S., Xu, K., and Blair, I. A. (1999) Covalent modification of 2′-deoxyguanosine by 4-oxo-2-nonenal, a novel product of lipid peroxidation. *Chem. Res. Toxicol. 12*, 1195−1204.

(9) Lee, S. H., Rindgen, D., Bible, R. H., Jr., Hajdu, E., and Blair, I. A. (2000) Characterization of 2′-deoxyadenosine adducts derived from 4-oxo-2-nonenal, a novel product of lipid peroxidation. *Chem. Res. Toxicol. 13*, 565−574.

(10) Rindgen, D., Lee, S. H., Nakajima, M., and Blair, I. A. (2000) Formation of a substituted 1,N^2-etheno-2′-deoxyadenosine adduct by lipid hydroperoxide-mediated generation of 4-oxo-2-nonenal. *Chem. Res. Toxicol. 13*, 846−852.

(11) Lee, S. H., Oe, T., and Blair, I. A. (2002) 4,5-Epoxy-2(E)-decenal-induced formation of 1,N^6-etheno-2′-deoxyadenosine and 1,N^2-etheno-2′-deoxyguanosine adducts. *Chem. Res. Toxicol. 15*, 300−304.

(12) Lee, S. H., Arora, J. S., Oe, T., and Blair, I. A. 4-Hydroperoxy-2-nonenal-induced formation of 1,N^2-etheno-2′-deoxyguanosine adducts. *Chem. Res. Toxicol.* Submitted for publication.
(13) Lee, S. H., and Blair, I. A. (2001) Oxidative DNA damage and cardiovascular disease. *Trends Cardiovasc. Med. 11*, 148−155.
(14) Pryor, W., and Porter, N. A. (1990) Suggested mechanisms for the production of 4-hydroxy-2-nonenal from the autoxidation of polyunsaturated fatty acid. *Free Radical Biol. Med. 8*, 541−543.
(15) Funk, C. D. (2001) Prostaglandins and leukotrienes: Advances in eicosanoid biology. *Science 294*, 1871−1875.
(16) Sun, M., Deng, Y., Batyreva, E., Sha, W., and Salomon, R. G. (2002) Novel bioactive phospholipids: Practical total syntheses of products from the oxidation of arachidonic and linoleic esters of 2-Lysophosphatidylcholine. *J. Org. Chem. 67*, 3575−3584.
(17) Spanbroek, R., Grabner, R., Lotzer, K., Hildner, M., Urbach, A., Ruhling, K., Moos, M. P., Kaiser, B., Cohnert, T. U., Wahlers, T., Zieske, A., Plenz, G., Robenek, H., Salbach. P., Kuhn, H., Radmark, O., Samuelsson, B., and Habenicht, A. J. (2003) Expanding expression of the 5-lipoxygenase pathway within the arterial wall during human atherogenesis. *Proc. Natl. Acad. Sci. U.S.A. 100*, 1238−1243.
(18) Mehrabian, M., Allayee, H., Wong, J., Shi, W., Wang, X. P., Shaposhnik, Z., Funk, C. D., Lusis, A. J., and Shih, W. (2002) Identification of 5-lipoxygenase as a major gene contributing to atherosclerosis susceptibility in mice. *Circ. Res. 91*, 120−126.
(19) Guevara, N. V., Chen, K. H., and Chan, L. (2001) Apoptosis in atherosclerosis: Pathological and pharmacological implications. *Pharmacol. Res. 44*, 59−71.
(20) Geng, Y. J., and Libby, P. (2002) Progression of atheroma: a struggle between death and procreation. *Arterioscler. Thromb. Vasc. Biol. 22*, 1370−1380.
(21) Hankin, J. A., Jones, D. N., and Murphy, R. C. (2003) Covalent binding of leukotriene A4 to DNA and RNA. *Chem. Res. Toxicol. 16*, 551−561.
(22) Schneider, C., Tallman, K. A., Porter, N. A, and Brash, A. R. (2001) Two distinct pathways of formation of 4-hydroxynonenal. Mechanisms of nonenzymatic transformation of the 9- and 13-hydroperoxides of linoleic acid to 4-hydroxyalkenals. *J. Biol. Chem. 276*, 20831−20838.
(23) Uchida, K. (2003) 4-Hydroxy-2-nonenal: A product and mediator of oxidative stress. *Prog. Lipid Res. 42*, 318−343.
(24) Frimer, A. A. (1979) The reaction of singlet oxygen with olefins: the question of mechanism. *Chem. Rev. 79*, 359−367.
(25) Gardner, H. W., and Plattner, R. D. (1984) Linoleate hydroperoxides are cleaved heterolytically into aldehydes by a Lewis acid in aprotic solvent. *Lipids 19*, 294−298.
(26) Gardner, H. W., and Hamberg, M. (1993) Oxygenation of 3(Z)-nonenal to 2(E)-4-hydroxy-2-nonenal in the broad bean (Vicia faba L.). *J. Biol. Chem. 268*, 6971−6977.
(27) Buettner, G. R. (1993) The pecking order of free radicals and antioxidants: Lipid peroxidation, α-tocopherol, and ascorbate. *Arch. Biochem. Biophys. 300*, 535−543.
(28) Linn, S. (1998) DNA damage by iron and hydrogen peroxide in vitro and in vivo. *Drug Metab. Rev. 30*, 313−326.
(29) Burcham, P. C. (1998) Genotoxic lipid peroxidation products: Their DNA damaging properties and role in formation of endogenous DNA adducts. *Mutagenesis 13*, 287−305.
(30) Vogelstein, B., Lane, D., and Levine, A. J. (2000) Surfing the p53 network. *Nature 408*, 307−310.
(31) Martinet, W., Knaapen, M. W., De Meyer, G. R., Herman, A. G., and Kockx, M. M. (2002) Elevated levels of oxidative DNA damage and DNA repair enzymes in human atherosclerotic plaques. *Circulation 106*, 927−932.
(32) Kockx, M. K., and Herman, A. G. (2000) Apoptosis in atherosclerosis: Beneficial or detrimental. *Cardiovasc. Res. 45*, 736−746.
(33) Pandya, G. A., and Moriya, M. (1996) 1,N^6-ethenodeoxyadenosine, a DNA adduct highly mutagenic in mammalian cells. *Biochemistry 35*, 11487−11492.
(34) Levine, R. L., Yang, I. Y., Hossain, M., Pandya, G. A., Grollman, A. P., and Moriya, M. (2000) Mutagenesis induced by a single 1,N^6-ethenodeoxyadenosine adduct in human cells. *Cancer Res. 60*, 4098−4104.

TX049693D